Nuclear Instruments and Methods in Physics Research A 606 (2009) 218–222

Contents lists available at ScienceDirect

Nuclear Instruments and Methods in Physics Research A

journal homepage: www.elsevier.com/locate/nima

Low-velocity ion slowing down in binary ionic mixtures

Bekbolat Tashev [a], Fazylkhan Baimbetov [a], Claude Deutsch [b,*], Patrice Fromy [c]

[a] Department of Physics, Kazakh National University, Tole Bi 96, Almaty 480012, Kazakhstan
[b] LPGP (UMR-CNRS 8578), Universite Paris XI, 91405 Orsay, France
[c] Direction de l'Informatique, Université Paris XI, 91405 Orsay, France

ARTICLE INFO

Available online 24 March 2009

Keywords:
Low velocity
Ion stopping
Binary ionic mixtures

ABSTRACT

We focus our attention on the low ion velocity stopping mechanisms in a multicomponent and dense target plasmas built of quasi-classical electron fluids neutralizing binary ionic mixtures such as deuterium–tritium of current fusion interest, proton-helium like iron in the solar interior or proton-helium ions considered in planetology, as well as other mixtures of fiducial concern in the heavy ion beam production of warm dense matter at Bragg peak conditions. The target plasma is taken in a multicomponent dielectric formulation à la Fried-Conte. We stress out the occurrence of projectile ion velocities (so-called critical) for which target electron slowing down equals that of the given target ion components.

The corresponding multi-quadrature computations, albeit rather heavy, can be monitored analytically through a very compact code operating a PC cluster.

Slowing down results are systematically scanned w.r.t. target temperature, electron density as well as ion composition.

1. Introduction

Recently, in many subfields of plasma physics, involving very dense and multicomponent plasmas, most of them built on low Z elements, one witnesses a specific focussed interest on low-velocity ion slowing down (LVISD). To name a few, let us first mention proton or possibly heavier ion stopping [1,2] considered in the selective heating of hot spots toward the goal of fast ignition in inertially confined fusion (ICF) through very intense and femtolaser produced ion beams [3–5]. The latter fortunately display a very effective current neutralization through comoving electron beams which leads to a very small transverse beam emittance. Up to now, most of the technical attention has been focussed on proton beams. Very recently [6], flyer acceleration techniques are expected to extend those performances to heavier projectiles, such as carbon, berylium or fluorine.

In the field of ICF, one is mostly motivated to trigger nuclear reactions within an arbitrary mixture of the hydrogen isotopes, such as deuterium and tritium. Usually, one currently stresses equiproportionality. However, recent studies advocating the so-called tritium lean fuels [7] demonstrate the attractiveness of a depleted tritium DT mixture, which allows, for instance, a significant reduction of the fuel beta-radioactivity. Fuel ignition being triggered by alpha particle stopping, the corresponding LIVSD, near the end of range, is supposed to be of great practical significance. Those considerations lead us to pay a special attention to proton (H^+) and alpha (He^{2+}) stopping in very dense and quasi-symmetric DT mixtures with corresponding electron density $10^{23} \leqslant n_e$ $(\mathrm{cm}^{-3}) \leqslant 10^{26}$ and equilibrated temperature $10 \leqslant T$ (eV) $\leqslant 20{,}000$.

The pertaining LIVSD should allow a fine tuning of the beam–target interaction involved in the fast ignition scenario (FIS). In addition to obvious and deep implications of low-velocity ion slowing down (LVISD) in FIS/ICF and some important areas in astrophysics [15,17], we also notice the present hot topic featuring the production of the so-called warm dense matter (WDM) through intense and low energy heavy ion beams stopped in thin films, in close vicinity of their Bragg peak [8,9], near the end of range.

The basic LIVSD behavior is, as well-known of the form

$$-\frac{\mathrm{d}E}{\mathrm{d}x} = A v_p \qquad (1)$$

in the low ion projectile velocity limit advocated previously with energy/nucleon $E/A \leqslant 100$ keV/amu.

The paper is organized as follows. Section 2 adapts the well-known dielectric formalism to an overall neutral binary ionic mixture (BIM) with electrons, taken as mostly classical (small $\hbar \neq 0$ effects).

Section 3 stresses basic LVISD trends in quasi-symmetric BIM such as the deuterium–tritium system. In this respect, a certain

* Corresponding author.
E-mail address: claude.deutsch@pgp.u-psud.fr (C. Deutsch).

0168-9002/$ - see front matter © 2009 Elsevier B.V. All rights reserved.
doi:10.1016/j.nima.2009.03.108

attention is given to the projectile velocity $v_{p,crit}$ at which target electron stopping equals target BIM stopping [10].

2. Basic formulation

Within the dielectric framework of present concern, we consider the electromagnetic response of a target plasma built on electrons and ion species (Z_i, M_i). The target ion part is taken here as a weakly coupled binary ionic mixture, which will prove sufficient in the subsequent considered plasma targets. In such an approach, it appears useful to work with the overall dielectric function

$$\varepsilon(\vec{k},\omega) = 1 + \frac{1}{k^2}\left(W\left(\frac{W}{k}\right) + W\left(\sqrt{M_1}\frac{W}{k}\right) + W\left(\sqrt{M_2}\frac{W}{k}\right)\right) \tag{2}$$

with the usual Fried–Conte dispersion function $W(\mathrm{Im}\,\zeta \geqslant 0)$

$$W(\varsigma) = \frac{1}{\sqrt{2\pi}} \lim_{\nu\to 0+} \int_{-\infty}^{\infty} \mathrm{d}x \frac{x e^{-x^2/2}}{x - \varsigma - i\nu} \tag{3}$$

and $X(\zeta) = \mathrm{Re}\, W(\zeta)$, $Y(\zeta) = \mathrm{Im}\, W(\zeta)$. Generalizing linearly through expression (2) the standard one-component stopping quadrature [11,12]

$$-\left[\frac{\mathrm{d}E}{\mathrm{d}x}\right] = \frac{Z^2 N_D}{(2\pi)^2} \int_0^{k_{max}} \mathrm{d}k\, k^3 \int_{-1}^{+1} \mathrm{d}\mu \frac{\mu Y(\mu v_p)}{[k^2 + X(\mu v_p)]^2 + Y^2(\mu v_p)} \tag{4}$$

with $Z = Z_{eff}/N_D$, where Z_{eff} denotes the projectile effective charge at velocity v_p, $N_D = n_e \lambda_{De}^3$ in terms of target electron density and corresponding Debye length. In the sequel, v_p will be scaled by $v_{the} = \sqrt{k_B T/m_e}$, thermal electron velocity with T, thermalized target temperature. In Eq. (4), we have to pay attention to the selection of maximum cutoff k_{max}, taking into account quantum effects diffraction ($k_B T \geqslant 1\mathrm{Ry}$) in a high-temperature plasma. So, one explicits [11,12]

$$k_{max} = \mathrm{Min}\left(\frac{m(v_p^2 + v_{the}^2)}{Z_{eff} e^2}, \frac{2m\sqrt{v_p^2 + v_{the}^2}}{\hbar}\right)$$
$$= \mathrm{Min}\left(\frac{4\pi}{Z}(v_p^2 + 2), 8\pi\sqrt{2N_D}\frac{\alpha c}{v_{the}}\sqrt{v_p^2 + 2}\right) \tag{5}$$

where v_p is now dimensionless on the second line on the right-hand side. $\alpha = 1/137$ is the fine structure constant, and c, light velocity. In this regard, it should be noticed that the occurrence of quantum diffraction k_{max} is restricted to the electron fluid component of the target. The corresponding BIM will always appear as pointlike classical, as long as one restricts to the velocity range $v_{thi} \leqslant v_p \leqslant v_{the}$. In adapting Eq. (4) to BIM stopping, it proves convenient to introduce the relative ion concentration of species 1, i.e.

$$\alpha = \frac{N_1}{N_1 + N_2} \tag{6}$$

in terms of ion number N_i with $i = 1,2$, in target plasma, so that BIM densities

$$n_1 = \frac{n_e \alpha}{\bar{Z}}, \quad n_2 = \frac{n_e(1-\alpha)}{\bar{Z}}, \quad \bar{Z} = Z_1\alpha + Z_2(1-\alpha) \tag{7}$$

are straightforwardly expressed in terms of electron density n_e.

Then, we can estimate the stopping contributions of every target component: electron (0), ion 1 and ion 2 as follows:

$$-\frac{\mathrm{d}E_0}{\mathrm{d}x} = C_0 \int_{-1}^{+1} \mathrm{d}\mu \frac{\mu Y[\mu v]}{D[k,\mu v]} \tag{8a}$$

$$-\frac{\mathrm{d}E_1}{\mathrm{d}x} = C_1 \int_0^{k_{max_1}} \mathrm{d}k\, k^3 \int_{-1}^{+1} \mathrm{d}\mu \frac{\mu Y[\sqrt{M_1}\mu v]}{D[k,\mu v]} \tag{8b}$$

$$-\frac{\mathrm{d}E_2}{\mathrm{d}x} = C_2 \int_{-1}^{+1} \mathrm{d}\mu \frac{\mu Y[\sqrt{M_2}\mu v]}{D[k,\mu v]} \tag{8c}$$

where

$$D[k,\mu v] = \left(k^2 + X[\mu v] + X\left[\sqrt{M_1}\mu v\right] + X\left[\sqrt{M_2}\mu v\right]\right)^2 + \left(Y[\mu v] + Y\left[\sqrt{M_1}\mu v\right] + Y\left[\sqrt{M_2}\mu v\right]\right)^2 \tag{9}$$

$$C_0 = \frac{k_B T Z_{eff}^2}{4\pi^2 n_e \lambda_{De}^4} \tag{10a}$$

$$C_1 = \frac{C_0 Z_1^4 \alpha}{\bar{Z}} \tag{10b}$$

$$C_2 = \frac{C_0 Z_2^4 (1-\alpha)}{\bar{Z}}, \tag{10c}$$

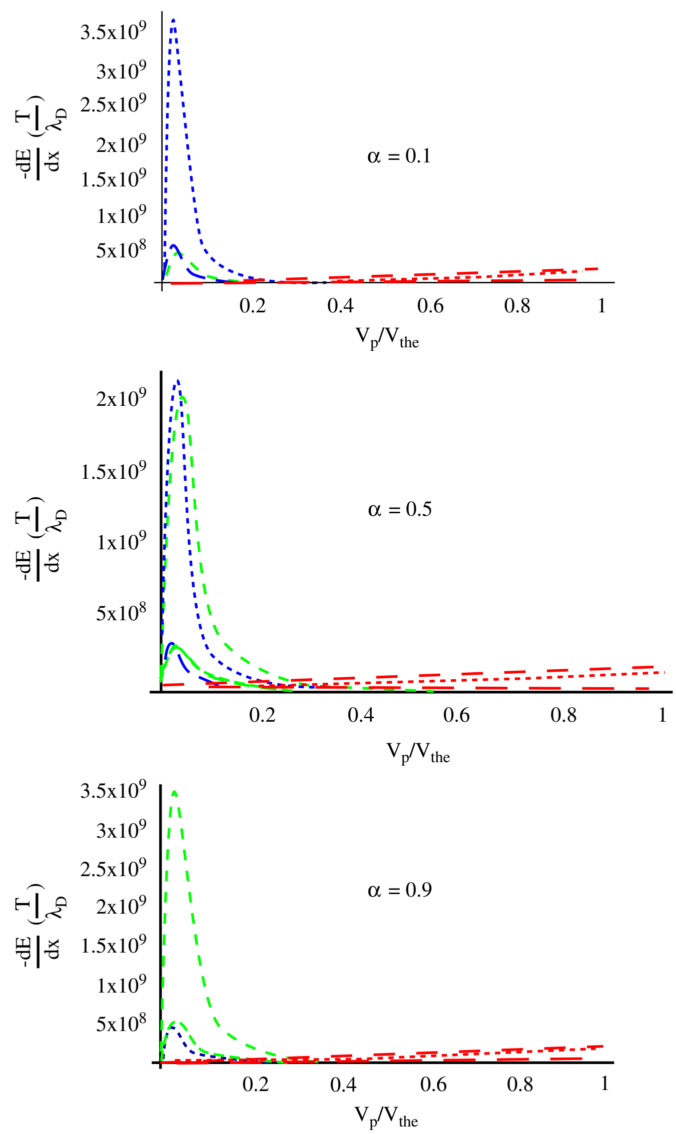

Fig. 1. Proton stopping in H^+–D^+ BIM in terms of v_p/v_{the}. $n_e = 10^{23}\,\mathrm{e\,cm^{-3}}$ alpha denotes proton concentration in BIM. T(eV) = ……… 10, - - - - - 100, – – – 1000. Red pertains to e-stopping, green to H^+-stopping and blue to D^+-stopping.